Journal of Theoretical Biology 462 (2019) 122–133

Contents lists available at ScienceDirect

Journal of Theoretical Biology

journal homepage: www.elsevier.com/locate/jtb

Interaction between epidemic spread and collective behavior in scale-free networks with community structure

Zhongpu Xu[a], Kezan Li[b], Mengfeng Sun[a], Xinchu Fu[a,*]

[a] Department of Mathematics, Shanghai University, Shanghai 200444, China
[b] School of Mathematics and Computing Science, Guilin University of Electronic Technology, Guilin 541004, China

ARTICLE INFO

Article history:
Received 6 June 2018
Revised 28 October 2018
Accepted 4 November 2018
Available online 10 November 2018

Keywords:
Community network
Epidemic spread
Cluster synchronization
Epidemic threshold
Global stability

ABSTRACT

Many real-world networks exhibit community structure: the connections within each community are dense, while connections between communities are sparser. Moreover, there is a common but non-negligible phenomenon, collective behaviors, during the outbreak of epidemics, are induced by the emergence of epidemics and in turn influence the process of epidemic spread. In this paper, we explore the interaction between epidemic spread and collective behavior in scale-free networks with community structure, by constructing a mathematical model that embeds community structure, behavioral evolution and epidemic transmission. In view of the differences among individuals' responses in different communities to epidemics, we use nonidentical functions to describe the inherent dynamics of individuals. In practice, with the progress of epidemics, individual behaviors in different communities may tend to cluster synchronization, which is indicated by the analysis of our model. By using comparison principle and Geršgorin theorem, we investigate the epidemic threshold of the model. By constructing an appropriate Lyapunov function, we present the stability analysis of behavioral evolution and epidemic dynamics. Some numerical simulations are performed to illustrate and complement our theoretical results. It is expected that our work can deepen the understanding of interaction between cluster synchronization and epidemic dynamics in scale-free community networks.

1. Introduction

Complex networks are widely used to quantify and predict complex systems in various disciplines, such as electricity and transportation systems (Dharmaweera et al., 2015; Orosz et al., 2010), biological systems (Khan et al., 2015; Vidal et al., 2011), economic and financial systems (Garas et al., 2010; Vitali et al., 2011), and social systems (Barabási, 2007; Watts, 2007). This has inspired great interest in developing mathematical models that can capture general network attributes (Boccaletti et al., 2006). In addition, using the actual data to reconstruct networks, from which we can derive some properties and make a prediction for future events (Duarte et al., 2007). Therefore, the study of complex networks is crucial to the observation of realistic systems.

The study of complex networks can be divided into several categories (Boccaletti et al., 2006; Golubitsky and Stewart, 2006; Newman, 2012), such as the topological structure of complex networks, the propagation dynamics in complex networks, etc. With regard to the latter, propagation dynamics in complex networks include disease transmission (Keeling and Eames, 2005; Newman, 2002), packet delivery (Arenas et al., 2001; Ohira and Sawatari, 1998), rumor propagation (Moreno et al., 2004; Zanette, 2002), and computer virus spread (Liebovitch and Schwartz, 2003; Newman et al., 2002). Epidemic spread has been one of the richest fields in the dynamics of complex networks (Boguñá et al., 2013). In an epidemic network, each individual is equivalent to a node, and the interaction between individuals can be realized through links in this network.

In recent years, the propagation process of epidemics in single or multiple contact networks has been widely studied (Liu et al., 2003; Wang et al., 2016). However, with the rapid development of information technology, many high-tech products have entered our daily life, which can make people contact with others not only in real life, but also in online social networks, leading to extensive information exchange among individuals. In the information age, the problems concerning the propagation of epidemics have become very complicated. In addition to epidemic spread, there are also online and offline information dissemination simultaneously. In particular, when the partial entities in these two processes are identical, the spread of epidemics would be affected by information diffusion. For example Kan and Zhang (2017), during

* Corresponding author.
E-mail addresses: xcfu@shu.edu.cn, x.c.fu@163.com (X. Fu).

https://doi.org/10.1016/j.jtbi.2018.11.003
0022-5193/

a flu season, when an individual gets the flu, he/she may transmit the information on influenza through Facebook or Twitter. His/Her friends will be informed to reduce the risk of infection by injecting flu vaccine or avoiding close contact with their neighbors. In real-world networks, if more susceptible individuals are informed of epidemic information, their awareness of protection will increase correspondingly, which make people change their behaviors such that the outbreak of infectious diseases can be effectively controlled or even disappeared (Funk et al., 2009).

It is noteworthy that many complex networks are scale-free (Barabási, 2007; Barabási and Bonabeau, 2003), which mean that the degree distribution of these networks follows the power-law form $P(k) \sim k^{-\gamma}$, where $P(k)$ is the probability that a node in networks is connected to k other nodes, and γ is a positive real number determined by a given network. The power-law distribution can lead to scale-free behaviors, such as short distance, because of there may be hubs or nodes with large degrees. The analysis on the epidemic models in scale-free networks has revealed the importance of topology for transmission dynamics, such as the lack of epidemic threshold (Boguñá et al., 2003).

On the other hand, most real-world networks display the community structure (Girvan and Newman, 2002; Newman, 2006). That is, there are groups of nodes with close inter-connections, and few connections with the nodes outside the group. The community may be classmates, friends, colleagues, club members, etc. How community structure affects network dynamics is still a problem worth exploring. For example, the community structure of networks affects the cooperative process in real-world networks (Lozano et al., 2008). Recent studies have found that community structure plays an important role in the process of epidemic spread in networks, which is referred to the networks with non-overlapping communities (Chu et al., 2009; Huang and Li, 2007). It has been shown that the community structure influences the epidemic threshold, epidemic prevalence and information lifetime in complex networks. Although the community structure affects the process of epidemic spread in networks, the extent to which the community structure affects epidemics in practical networks has been largely unexplained.

Recently, researches between the spread of epidemics and the dynamics of human behaviors have been very prevalent (Funk et al., 2010; Verelst et al., 2016; Zhang et al., 2017), and they have their own innovations and understanding in these studies. However, in the underlying structure of the dynamics, they all made a relatively crude hypothesis. The models without network structure are usually based on the assumption of homogeneous mixing (Cai et al., 2015; Kumar et al., 2017), even in the case of networked models, these two kinds of dynamics are also studied on the whole network (Wu et al., 2012; Zhang et al., 2014), however, the structures of which may be different. Obviously, it is very rough and ignores the differences of the underlying structures, which may have a significant impact on these two sorts of dynamics. Therefore, it is necessary for us to make a detailed division of the network.

Based on the discussion above, we consider the interaction between epidemic spread and population behaviors (which may tend to synchronization under certain conditions) in the context of scale-free community networks. Similar studies on interaction between epidemic spread and human behaviors have been shown in Li et al. (2011, 2012) and Sun et al. (2017). Li et al. investigated the effects of human behaviors on epidemic dynamics based on the heterogeneous mean-field theory, and further discussed the control of the epidemic (Li et al., 2011; 2012). Sun et al. set the underlying network as quenched and introduced time delays (epidemic delay and coupling delay) to study the effects of protective behaviors and delays on epidemic dynamics (Sun et al., 2017). On the basis of the above researches, we reduce the restrictions caused by some hypotheses. For example, we not only adopt a more accurate theory — quenched mean-field (QMF) theory, but also consider the bi-directional feedback. Most importantly, we classify individuals in underlying networks into different groups according to the characteristics of natural regions and propagation dynamics, i.e., we incorporate the community structure into our model. Our main goal is to enhance our understanding of interaction dynamics in the setting of community networks.

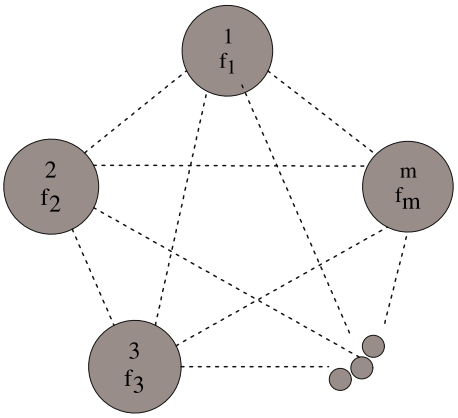

Fig. 1. The community structure of a complex network. The ith community in this network is denoted by the ith numbered gray circle, with local dynamics f_i. The dotted lines show the probable connections between the m communities.

In this paper, we consider the following situation (see Fig. 1): the whole population is consisting of N individuals, which is distributed over m ($2 \le m < N$) communities. The inter-connection pattern of mth community is described by an $N_m \times N_m$ matrix, where N_m represents the number of nodes in mth community. In addition to the m matrices, the remaining elements of the adjacency matrix A indicate whether there is a connection between the elements of different communities.

Let σ_i denotes the σ_ith community in which node i lies, and $1 \le \sigma_i \le m, \quad i = 1, 2, \ldots, N$. The set of all nodes in the σ_ith community is denoted by $\mathcal{N}_{\sigma_i}$, and the cardinal number of $\mathcal{N}_{\sigma_i}$ is denoted by N_{σ_i}. So, if $j \in \mathcal{N}_k, 1 \le j \le N, 1 \le k \le m$, then $\sigma_j = k$.

For simplicity, and in order to more intuitive see each node in the community, we give the following vector to show any node i belongs to its community (This can always be done by renumbering the nodes):

$$(1, 2, \ldots, N) = (\overbrace{1, \ldots, N_1}^{first\ community}, \overbrace{N_1 + 1, \ldots, N_1 + N_2}^{second\ community}, \ldots, \overbrace{N - N_m + 1, \ldots, N}^{m\text{th } community}),$$

where $N = N_1 + \ldots + N_m$.

We present a graphical representation of a complex network with community structure in Fig. 1. We use f_i to denote the local dynamics of all nodes in the ith community, with each node being an n-dimensional dynamical system.

Each community can be regarded as a local population containing two types of individuals: S (susceptible) and I (infected). Each infected node becomes susceptible with rate δ, and each susceptible node has a probability ν of contagion by contacting with each infected neighbor. So, we define the effective infection rate $\lambda = \nu/\delta$. In this paper, we consider the standard SIS model in a quenched network of size N, i.e., the community networks are embedded in the quenched network. Let $\rho_i(t)$ be the infection density of node i at time t. For simplicity, we suppose that the degree is uncorrelated in the network, then the evolution equation of node i

can be written by

$$\dot{\rho}_i(t) = -\rho_i(t) + \lambda\phi_{\sigma_i}(t)[1-\rho_i(t)]\sum_{j=1}^{N} a_{ij}\rho_j(t),\ \ i = 1, 2, \ldots, N, \tag{1}$$

where a_{ij} is an element of the adjacency matrix, defining as follows: if nodes i and j are connected, then $a_{ij} = 1$, or $a_{ij} = 0$ otherwise, and the disease prevalence $\rho(t) = \sum_{i=1}^{N} \rho_i(t)/N$. The term $\phi_{\sigma_i}(t)$ denotes the information of synchronization or infection control behavior of individuals, and more details will be given later.

The state equation of individual behaviors can be described by

$$\dot{x}_i(t) = f_{\sigma_i}(x_i(t)) - c_{\sigma_i}(t)\sum_{j=1}^{N} l_{ij}\Gamma x_j(t),\ \ i = 1, 2, \ldots, N, \tag{2}$$

where $x_i(t) = (x_{i1}(t), x_{i2}(t), \ldots, x_{in}(t))^T \in \mathbb{R}^n$ is the state variable of the node i at time $t \in [0, +\infty)$. The function $f_{\sigma_i} : \mathbb{R}^n \to \mathbb{R}^n$ describes the local dynamics for nodes in the σ_ith community and shows ample dynamical behaviors, which is supposed to be chaotic. The local dynamics for all nodes in each community are the same, and any two nodes from different communities have different local dynamics. Obviously, if $\sigma_i \neq \sigma_j$, i.e., node i and j are geared to different communities, then $f_{\sigma_i} \neq f_{\sigma_j}$. $c_{\sigma_i}(t) > 0$ denotes the time varying coupling strength in the σ_ith community that can be adjusted. $\Gamma = diag(\gamma_1, \gamma_2, \ldots, \gamma_n) \in \mathbb{R}^{n\times n}$ represents the inner-coupling matrix, which is supposed to be a diagonal matrix with $\gamma_i \geq 0$. The Laplacian matrix of the whole network $L = (l_{ij})_{N\times N}$ is defined as follows: if node i and node $j (i \neq j)$ are linked by an edge, then $l_{ij} = l_{ji} = -1$; otherwise, $l_{ij} = l_{ji} = 0$, and the diagonal elements of the Laplacian matrix L are defined as follows:

$$l_{ii} = -\sum_{\substack{j=1\\ j\neq i}}^{N} l_{ij} = -\sum_{\substack{j=1\\ j\neq i}}^{N} l_{ji} = k_i, \quad i = 1, 2, \ldots, N, \tag{3}$$

where k_i denotes the degree of node i.

Moreover, we assume that L is an irreducible matrix, it induces the eigenvalues of matrix L to satisfy $0 = \lambda_1 < \lambda_2 \leq \ldots \leq \lambda_N$. Hence, by (3) and matrix theory, there exists a unitary matrix U such that $L = U\Lambda U^T$, where $U^T U = I$ and $\Lambda = diag(\lambda_1, \lambda_2, \ldots, \lambda_N)$.

In the light of the above analyses, in this paper, we construct an interactive mathematical model characterizing epidemic spread and human behaviors in scale-free community networks. Then, we analyze the impact of cluster synchronization and community structure on epidemiological dynamics.

The remainder of this paper is organized as follows. In Section 2, we establish an epidemic synchronization model in quenched community networks. In Section 3, we investigate the epidemic threshold of spreading dynamics network and perform the stability analysis of synchronization and transmission dynamics. Some numerical simulations are presented in Section 4. Finally, Section 5 concludes the whole work.

2. Epidemic synchronization model in community networks

In our epidemic networks with community structure, information spreading is accompanied by the spread of infectious diseases, which can induce individuals spontaneously to reduce the frequency of physical contact with infected individuals and take the protective measures. That means the rate of the change of the coupling strength $\dot{c}_{\sigma_i}(t)$ in the σ_ith community is directly proportional to the infection density $\rho_{\sigma_i}(t)$ of the corresponding community. On the other hand, when the collective self-protection behavior is prevalent, the communication of disease information and protective measures among individuals will become stable as they have reached an agreement. Hence, the proportional relation between $\dot{c}_{\sigma_i}(t)$ and the synchronization error $\sum_{j\in\mathcal{N}_{\sigma_i}} e_j^T(t)e_j(t)$ remains valid.

Based on the above assumptions and the traditional models (1) and (2), we can construct the following SIS epidemic cluster synchronization model:

$$\begin{cases} \dot{x}_i(t) = f_{\sigma_i}(x_i(t)) - c_{\sigma_i}(t)\sum_{j=1}^{N} l_{ij}\Gamma x_j(t), \\ \dot{\rho}_i(t) = -\rho_i(t) + \lambda\phi_{\sigma_i}(t)[1-\rho_i(t)]\sum_{j=1}^{N} a_{ij}\rho_j(t), \\ \dot{c}_{\sigma_i}(t) = \beta\rho_{\sigma_i}(t)\sum_{j\in\mathcal{N}_{\sigma_i}} e_j^T(t)e_j(t), \end{cases} \tag{4}$$

where $i = 1, 2, \ldots, N$. Besides, we define the additional term $\phi_{\sigma_i}(t) = (1-\alpha)E_{\sigma_i}(t) + \alpha$ in Eq. (1) with constant $\alpha \in (0,\ 1)$, where

$$E_{\sigma_i}(t) = \frac{1}{N_{\sigma_i}}\sum_{j\in\mathcal{N}_{\sigma_i}} \frac{\|s_{\sigma_i}(t) - x_j(t)\|^2}{1 + \|s_{\sigma_i}(t) - x_j(t)\|^2} \in [0, 1),$$

and $s_{\sigma_i}(t)$ is the synchronous state of the dynamical behavior network in the σ_ith community. Moreover, we can define the error variables $e_i(t) = x_i(t) - s_{\sigma_i}(t),\ \ i = 1, 2, \ldots, N$, and $\tilde{E}_{\sigma_i}(t) = \sum_{j\in\mathcal{N}_{\sigma_i}} \|s_{\sigma_i}(t) - x_j(t)\|^2 = \sum_{j\in\mathcal{N}_{\sigma_i}} e_j^T(t)e_j(t)$, the parameter $\beta > 0$, and $\rho_{\sigma_i}(t) = \sum_{j\in\mathcal{N}_{\sigma_i}} \rho_j(t)/N_{\sigma_i}$ denotes the disease prevalence of the σ_ith community. There are m communities in the network, so $E(t) = \sum_{j=1}^{N} \|s_{\sigma_j}(t) - x_j(t)\|^2 = \sum_{j=1}^{N} e_j^T(t)e_j(t) = \sum_{j\in\mathcal{N}_1} e_j^T(t)e_j(t) + \ldots + \sum_{j\in\mathcal{N}_m} e_j^T(t)e_j(t)$.

Moreover, the term $\phi_{\sigma_i}(t)$ in Eq. (1) means the admission rate (Wu et al., 2012), it can be considered as the prevalence of individual awareness or risk perception of the disease. When all individuals in different communities achieve synchronization, that is $E_{\sigma_i}(t) \to 0$ as $t \to \infty$, then $\phi_{\sigma_i}(t)$ is the minimum α. If the value of parameter α is smaller, i.e., the admission rate is smaller, then the individuals have the greater awareness to human collective behaviors to avoid being infected. Otherwise, there is no reaction in the population to the information of synchronization if $\alpha = 1$.

The variable $\phi_{\sigma_i}(t)$ also can be quantified as the infection control behavior of all individuals within each community, i.e., self-protection behaviors taken by individuals can reduce the likelihood of infection to a certain extent, such as washing hands and wearing face masks. So, the infection rate ν of each susceptible node becomes $\phi_{\sigma_i}(t)\nu$, then the effective infection rate λ becomes $\phi_{\sigma_i}(t)\lambda$, and the infection rate is smaller. Moreover, the above individual behaviors can be observed by others, it is easier to be accepted and more people likely tend to follow them, then there is a collectivization of behaviors. Thus, the dynamical behavior of parameter $\phi_{\sigma_i}(t)$ displays a synchronization, which could influence the epidemic dynamics.

Here, $\dot{s}_{\sigma_i}(t) = f_{\sigma_i}(s_{\sigma_i}(t))$ describes the identical local dynamics for all nodes in the σ_ith community. The dynamical network achieves synchronization if

$$\lim_{t\to+\infty} \|e_i(t)\| = 0, \quad i = 1, 2, \ldots, N, \tag{5}$$

that is any node in σ_ith community synchronizes to the corresponding dynamic state $s_{\sigma_i}(t)$. So, we can define a set $\Psi = (s_{\sigma_1}, s_{\sigma_2}, \ldots, s_{\sigma_N}) \subset \mathbb{R}^{n\times N}$ as the cluster synchronization manifold for the network (2). Moreover, the synchronization manifold is stable when condition (5) holds, i.e., spreading induced synchronization.

3. Stability analysis of global synchronization and spreading dynamics

Predicting the epidemic threshold is an important issue for studying the epidemic spreading in networks. Now, we give the following Theorem to determine the epidemic threshold of the epidemic spreading network in model (4).

Theorem 1. *For the epidemic spreading network in model (4), if an epidemic spreads and becomes endemic, then it is necessarily true that* $\lambda > \lambda_c = 1/\alpha\rho(A)$, *where* $\rho(A)$ *is the spectral radius of the matrix* $A = (a_{ij})_{N\times N}$, $i, j = 1, 2, \ldots, N$.

Proof. From Eq. (1) and $\phi_{\sigma_i}(t) \geq \alpha > 0$, we obtain

$$\begin{aligned}\dot{\rho}_i(t) &= -\rho_i(t) + \lambda\phi_{\sigma_i}(t)[1-\rho_i(t)]\sum_{j=1}^{N} a_{ij}\rho_j(t)\\ &\geq -\rho_i(t) + \lambda\alpha[1-\rho_i(t)]\sum_{j=1}^{N} a_{ij}\rho_j(t),\end{aligned}$$

where $i = 1, 2, \ldots, N$.

Now, we can consider the equation

$$\dot{\rho}_i(t) = -\rho_i(t) + \lambda\alpha[1-\rho_i(t)]\sum_{j=1}^{N} a_{ij}\rho_j(t). \tag{6}$$

Then, we calculate the steady-state probability of infection for each node i from Eq. (6), denoted by ρ_i, which is determined by the following equation

$$\rho_i = \frac{\lambda\alpha\sum_j a_{ij}\rho_j}{1+\lambda\alpha\sum_j a_{ij}\rho_j}, \quad i = 1, 2, \ldots, N. \tag{7}$$

Letting $\Theta = \sum_{j=1}^{N} a_{ij}\rho_j$, then $\rho_i = \frac{\lambda\alpha\Theta}{1+\lambda\alpha\Theta}$, and we obtain a self-consistency equation:

$$\Theta = \sum_j a_{ij}\frac{\lambda\alpha\Theta}{1+\lambda\alpha\Theta} \equiv f(\Theta). \tag{8}$$

Obviously, $\Theta = 0$ is always a solution of Eq. (8), i.e., $f(0) = 0$. And,

$$f'(\Theta) = \sum_j a_{ij}\frac{\lambda\alpha}{(1+\lambda\alpha\Theta)^2} > 0,$$

$$f''(\Theta) = \sum_j a_{ij}\frac{-2\lambda^2\alpha^2}{(1+\lambda\alpha\Theta)^3} < 0,$$

thus, a nontrivial solution exists only if

$$\begin{aligned}\frac{df(\Theta)}{d\Theta}|_{\Theta=0} &= \sum_j a_{ij}\frac{\lambda\alpha}{(1+\lambda\alpha\Theta)^2}|_{\Theta=0}\\ &= \sum_j \lambda\alpha a_{ij} > 1.\end{aligned} \tag{9}$$

So we have

$$\lambda > 1/\alpha\sum_j a_{ij}. \tag{10}$$

Since the values of $\Sigma_j a_{ij}$ are related to i, so

$$\lambda > \frac{1}{\alpha\max_i\{\sum_j a_{ij}\}}. \tag{11}$$

From the above inequality, there exists $k \in \{1, 2, \ldots, N\}$, such that the solution $\bar{\rho}_k > 0$ for the system (6).

According to the matrix $A = (a_{ij})_{N\times N}$, supposing that the N eigenvalues of the matrix are Λ_m, $m = 1, 2, \ldots, N$, from Geršgorin theorem (Zhang, 2010), we have

$$|\Lambda_m| \leq \max_i\left\{\sum_j a_{ij}\right\}, \quad m = 1, 2, \ldots, N. \tag{12}$$

So, we obtain

$$\max_m\{|\Lambda_m|\} \leq \max_i\left\{\sum_j a_{ij}\right\}. \tag{13}$$

Denote by $\rho(A)$ the spectral radius of the matrix A, then $\rho(A) = \max_m\{|\Lambda_m|\}$, and

$$\rho(A) \leq \max_i\left\{\sum_j a_{ij}\right\} \Rightarrow \frac{1}{\rho(A)} \geq \frac{1}{\max_i\left\{\sum_j a_{ij}\right\}}. \tag{14}$$

If $\lambda > \frac{1}{\alpha\rho(A)}$, there will be $\bar{\rho}_k > 0$. Thus, there exists a k, such that $\bar{\rho}_k > 0$. Therefore, according to the comparison principle, we know for the original Eq. (1), $\rho_k \geq \bar{\rho}_k > 0$. Then, when $\lambda > \frac{1}{\alpha\rho(A)}$, there exists $k \in \{1, 2, \ldots, N\}$, such that $\rho_k > 0$.

The value of λ satisfying the inequality defines the epidemic threshold of the epidemic spreading network, i.e.,

$$\lambda_c = \frac{1}{\alpha\rho(A)}.$$

The proof is therefore completed. □

Define

$$H = \{(\rho_1, \rho_2, \ldots, \rho_N) \in \mathbb{R}^N | 0 \leq \rho_i \leq 1, i = 1, 2, \ldots, N\},$$

and denote by H^0 the interior of H, and $\rho_0 = (0, 0, \ldots, 0) \in \mathbb{R}^N$. Now, the definition as follows: if there exists a constant $c \in (0, 1)$ such that $\liminf_{t\to\infty}\rho_i(t) > c$ for all i provided $(\rho_1(0), \rho_2(0), \ldots, \rho_N(0)) \in H^0$, the spreading network in system (4) is regarded as uniformly persistent in H^0. Then, we have the following stability result.

Theorem 2. *For the epidemic spreading network in system (4),* ρ_0 *is the unique disease-free equilibrium of the network and it is globally stable in* H *if* $\lambda < \frac{1}{\rho(A)}$, *otherwise* ρ_0 *is unstable and the network is uniformly persistent in* H^0 *if* $\lambda > \lambda_c = \frac{1}{\alpha\rho(A)}$.

Proof. Consider the Lyapunov function $V(t) = \frac{1}{2}\sum_{i=1}^{N}\rho_i^2(t)$. Calculating the derivative of $V(t)$ along the solution of Eq. (1) gives

$$\begin{aligned}\frac{dV(t)}{dt} &= \sum_{i=1}^{N}\rho_i(t)\dot{\rho}_i(t)\\ &= \sum_{i=1}^{N}\rho_i(t)\left[-\rho_i(t) + \lambda\phi_{\sigma_i}(t)[1-\rho_i(t)]\sum_{j=1}^{N} a_{ij}\rho_j(t)\right]\\ &\leq \sum_{i=1}^{N}\rho_i(t)\left[-\rho_i(t) + \lambda\sum_{j=1}^{N} a_{ij}\rho_j(t)\right]\\ &= \lambda\sum_{i,j=1}^{N} a_{ij}\rho_i(t)\rho_j(t) - \rho(t)^T\rho(t)\\ &= \lambda\rho(t)^T A\rho(t) - \rho(t)^T\rho(t)\\ &= \rho(t)^T\left[\lambda\frac{A+A^T}{2} - E_N\right]\rho(t),\end{aligned} \tag{15}$$

where $\rho(t) = (\rho_1(t), \rho_2(t), \ldots, \rho_N(t))^T$ and the matrix $A = (a_{ij})_{N\times N}$. From Eq. (15), we can get

$$\lambda_{\max}\left[\lambda\frac{A+A^T}{2} - E_N\right] = \lambda_{\max}\left(\lambda\frac{A+A^T}{2}\right) - 1 \leq \lambda\lambda_{\max}(A) - 1,$$

we know $\rho(A) = \lambda_{\max}(A)$, so $\lambda < \frac{1}{\rho(A)}$ leads to $\frac{dV(t)}{dt} \leq 0$. In addition, from (15) we get $\dot{V}(t) = 0$ if and only if $\rho(t) = 0$. Therefore, when $\lambda < \frac{1}{\rho(A)}$, the singleton $\{\rho_0\}$ is the only compact invariant subset of the set $\{\rho | \frac{dV(t)}{dt} = 0\}$. By LaSalle's invariance principle, ρ_0 is globally asymptotically stable in H.

From Theorem 1, if $\lambda > \frac{1}{\alpha\rho(A)}$, we can draw the conclusion that $\frac{dV(t)}{dt} > 0$ in a neighborhood of ρ_0 in H^0. Thus, the disease-free

equilibrium ρ_0 is unstable, and the instability implies the spreading network is uniformly persistent in H^0 by a similar discussion in Ref. Guo et al. (2006). □

Remark 1. *In the above analysis, there exist two critical values* $\frac{1}{\rho(A)}$ *and* $\frac{1}{\alpha\rho(A)}$ *in the epidemic spreading network. Through some simulations (Figs. 6–8), one can note that there is no backward bifurcation for the model when the effective infection rate changes between these two critical values. And, the epidemic threshold of the network is* λ_c.

The synchronous state in a community can be defined as $s_{\sigma_i}(t) = \frac{1}{N_{\sigma_i}}\sum_{j\in\mathcal{N}_{\sigma_i}} x_j(t)$. According to the above definition $e_i(t) = x_i(t) - s_{\sigma_i}(t)$ and Eq. (2), it is easy to obtain $\sum_{i=1}^{N} e_i(t) = 0$, and we can write the corresponding error system as

$$\dot{e}_i(t) = f_{\sigma_i}(x_i(t)) - f_{\sigma_i}(s_{\sigma_i}(t)) - c_{\sigma_i}(t)\sum_{j=1}^{N} l_{ij}\Gamma e_j(t), \tag{16}$$

where $i = 1, 2, \ldots, N$.

By letting $F(t) = (f_{\sigma_1}(x_1(t))^T - f_{\sigma_1}(s_{\sigma_1}(t))^T, \ldots, f_{\sigma_N}(x_N(t))^T - f_{\sigma_N}(s_{\sigma_N}(t))^T)^T$, $C(t) = (c_{\sigma_1}(t), \ldots, c_{\sigma_N}(t))^T$, and $e(t) = (e_1^T(t), \ldots, e_N^T(t))^T$, the system (16) can be rewritten as

$$\dot{e}(t) = F(t) - C(t)(L\otimes\Gamma)e(t), \tag{17}$$

where $\otimes$ is the Kronecker product.

Assumption 1. *Suppose that there exists a positive matrix* $P = diag(p_1, p_2, \ldots, p_n)$ *and a constant* $\xi > 0$, *the function* $f_{\sigma_i}(x_i(t))$ *satisfies the following inequality*

$$\begin{aligned}&(x(t) - s_i(t))^T P[f_i(x(t)) - f_i(s_i(t))]\\ &\quad\le \xi\,(x(t) - s_i(t))^T(x(t) - s_i(t)),\end{aligned} \tag{18}$$

for all $x(t), s_i(t)\in R^n$ *and* $t \ge 0$, $i = 1, 2, \ldots, m$.

Now, we have the following Theorem about the global stability for the synchronization manifold Ψ of the dynamical behavior network in system (4).

Theorem 3. *Suppose that* $\lambda_c = 1/\alpha\rho(A)$ *is the epidemic threshold of the spreading network in system (4). If* $\lambda > \lambda_c$, *then a unique endemic equilibrium* ρ^* *exists in the system, and it is globally asymptotically stable, i.e., the synchronization manifold* Ψ *of the dynamical network in system (4) is also globally asymptotically stable.*

Proof. See Appendix A. □

4. Numerical simulations

In this section, to illustrate the above theoretical results about the model of SIS epidemic synchronization network (4), some numerical examples are presented. We consider a network with three communities, and the Barabási–Albert(BA) scale-free network (Barabási and Albert, 1999) as the topological structure embedded in model (4). So, the network is composed of three BA networks(three communities), and the communities are randomly connected by a few edges. The BA network starts from initial nodes $m_0 = 4$ and adds a new node with $m = 3$ edges connecting to the existing nodes in each time step, the size is set as $N = 100$. We set the sizes of three communities are $N_1 = 20, N_2 = 30, N_3 = 50$, respectively, and they have the same BA network structure. The local dynamics f of all nodes in three communities are defined as the chaotic Lorenz system, chaotic Chen system, and chaotic Lü system, respectively. And denoted by f_1, f_2, and f_3 as their corresponding vector field function, respectively. The chaotic Lorenz oscillator, as the desired orbit, can be described by the system

$$\begin{cases}\dot{x}_1 = a(x_2 - x_1),\\ \dot{x}_2 = bx_1 - x_2 - x_1x_3,\\ \dot{x}_3 = x_1x_2 - cx_3,\end{cases} \tag{19}$$

where parameters $a = 10, b = 28, c = 8/3$.

The Chen system is

$$\begin{cases}\dot{y}_1 = d(y_2 - y_1),\\ \dot{y}_2 = ey_1 - y_1y_3 + fy_2,\\ \dot{y}_3 = y_1y_2 - gy_3,\end{cases} \tag{20}$$

where parameters $d = 35, e = -7, f = 28, g = 3$.

The Lü system is

$$\begin{cases}\dot{z}_1 = h(z_2 - z_1),\\ \dot{z}_2 = -z_1z_3 + kz_2,\\ \dot{z}_3 = z_1z_2 - lz_3,\end{cases} \tag{21}$$

where parameters $h = 36, k = 20, l = 3$.

Hence, we suppose the inner-coupling matrix $\Gamma = I_N$, the initial coupling strength $c(0) = 0.001$, $\beta = 0.01$, the initial condition $\rho_3(0) = 0.003$, $\rho_k(0) = 0$, $k = 4, \ldots, d_m$, where d_m is the maximum degree. Define the synchronization errors of the three communities in the network as $E_1^*(t) = \sum_{i=2}^{N_1}[x_1(t) - x_i(t)]^2/(N_1 - 1)$, $E_2^*(t) = \sum_{i=N_1+2}^{N_1+N_2}[x_{N_1+1}(t) - x_i(t)]^2/(N_2 - 1)$, and $E_3^*(t) = \sum_{i=N_1+N_2+2}^{N}[x_{N_1+N_2+1}(t) - x_i(t)]^2/(N_3 - 1)$, respectively. In this case, by the simulations we can obtain the total number of links in the network is 294, and the three BA networks with 24 edges connected them randomly.

We set $\alpha = 0.5$. In Fig. 2, the three communities have different initial infection densities, as the growth of time t, we get the epidemic prevalence $\rho(t)$ of the total network and three different communities converge to zero rapidly when the effective infection rate $\lambda = 0.01 < \frac{1}{\rho(A)}$, i.e., the disease will die out if $\lambda < \frac{1}{\rho(A)}$. In this case, the synchronization errors $E^*(t)$ in three communities do not coverage to zero, which imply the epidemic dynamics in the system cannot successfully induce the synchronization of individual behaviors under the small infection rate $\lambda = 0.01$. In addition, all the time-varying coupling strengths $c(t)$ of three communities reach the steady-state values.

From Fig. 3, we can see that the epidemic prevalence $\rho(t)$ of the total network and three different communities all reach a peak, then converge to the corresponding steady-state values, and $E^*(t)$ of three communities all have a small fluctuation, then converge to zero, which imply that the epidemic dynamics in the system can successfully induce the synchronization of individual behaviors with a larger infection rate $\lambda = 0.4 > \lambda_c = \frac{1}{\alpha\rho(A)}$. Moreover, the three coupling strengths $c(t)$ also reach the steady-state values. In Fig. 4, by increasing the infection rate to 0.6, one can see that the epidemic dynamics enhance the speed of synchronization, and $\rho(t)$ towards the higher steady-state values. The changes of the other variables are similar to Fig. 3. If the infection rate is larger, individuals may obtain more information about the disease and may feel more threatened, thus people may take their self-protection behaviors more urgently to reduce the risk of infection, such as washing hands and wearing face masks, etc. If more people are wearing face masks in public, and it is easier to be observed and accepted by others, then one is more likely to follow suit, and the speed of synchronization of individual behaviors will be faster.

In Fig. 5, we set $\lambda = 0.4$ and $\alpha = 1$, which means there is no awareness to the information of synchronization, and other variables are similar to that in Fig. 3. With respect to Fig. 3, the infection rate is larger in the figure, and all the epidemic prevalence $\rho(t)$ increase rapidly and toward the larger steady-state values. The synchronization errors $E^*(t)$ converge to zero faster, which imply that the epidemic dynamics can enhance the speed of synchronization with the infection rate. All coupling strengths $c(t)$ of three communities reach the different steady states. From simulations, we can conclude that the epidemic dynamics can successfully induce the synchronization when the epidemic spread in the

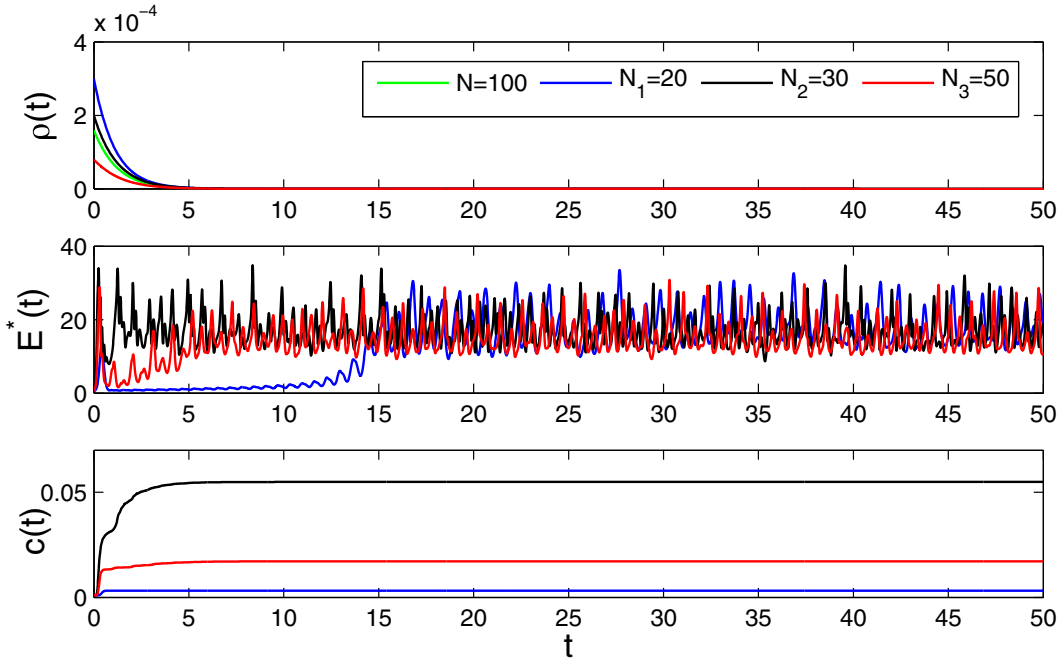

Fig. 2. When the infection rate $\lambda = 0.01 < 1/\rho(A)$, the time evolution of epidemic prevalence $\rho(t)$, synchronization error $E^*(t)$, and coupling strength $c(t)$ in model (4). The network is composed of three randomly connected BA scale-free networks with size $N_1 = 20, N_2 = 30, N_3 = 50$, respectively. The only green line denotes the epidemic prevalence of the total network in first subgraph, and $\rho(t)$, $E^*(t)$, $c(t)$ of three communities are described by blue, black, and red lines in three subgraphs, respectively. (For interpretation of the references to color in this figure legend, the reader is referred to the web version of this article.)

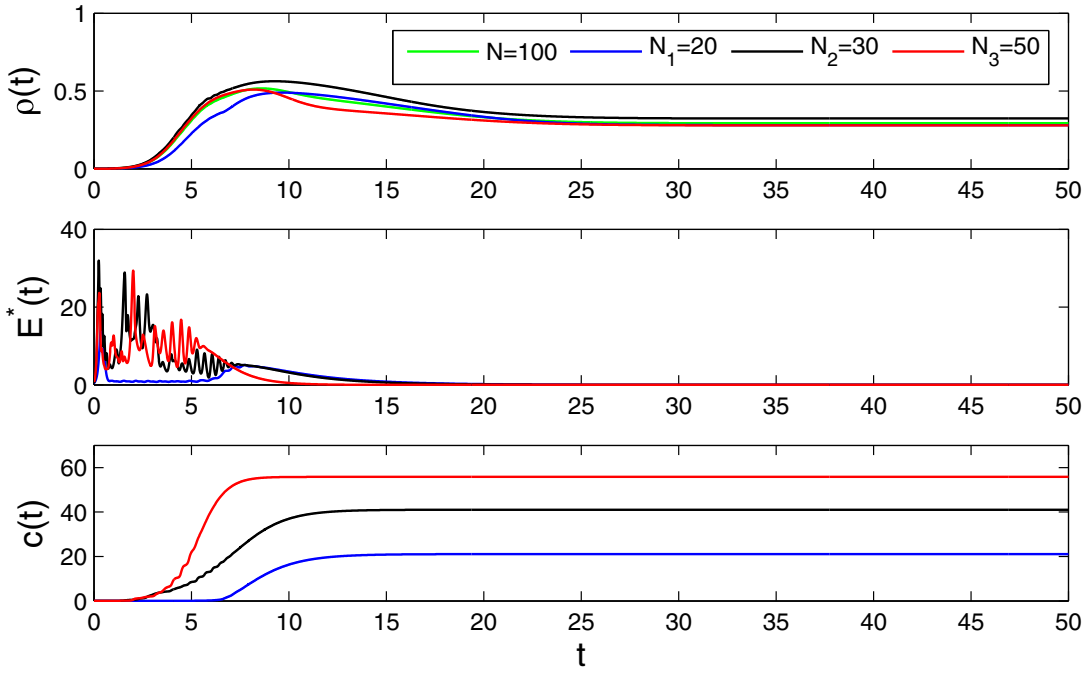

Fig. 3. When the infection rate $\lambda = 0.4 > \lambda_c$, the time evolution of $\rho(t)$, $E^*(t)$ and $c(t)$ in model (4). Line colors are similar to that shown in Fig. 2.

network. One can see that the numerical examples illustrate these theoretical results very well.

From the theoretical part, there exist two critical values in the spreading model, then we will verify whether the backward bifurcation exists in the model, which implies the existence of multiple endemic states. In Figs. 6 and 7, we set $\lambda = 0.145$ or $0.155 \in (\frac{1}{\rho(A)}, \frac{1}{\alpha\rho(A)})$ with different initial values, respectively. In these cases, the epidemic prevalence of the network converges to zero, which means the disease will die out. That is, there exists only the disease-free equilibrium in the model if $\lambda \in (\frac{1}{\rho(A)}, \frac{1}{\alpha\rho(A)})$, which is globally asymptotically stable. The synchronization errors in three communities do not coverage to zero, that is, the epidemic dynamics cannot successfully induce the synchronization of individual behaviors. Fig. 8 shows the relationship between the effective infection rate λ and the epidemic prevalence of the total network and three different communities. When λ reaches the critical value $\lambda_c = 0.189$, the plots all begin to rise, i.e., the disease begins to spread. The figure also ensure the epidemic threshold of

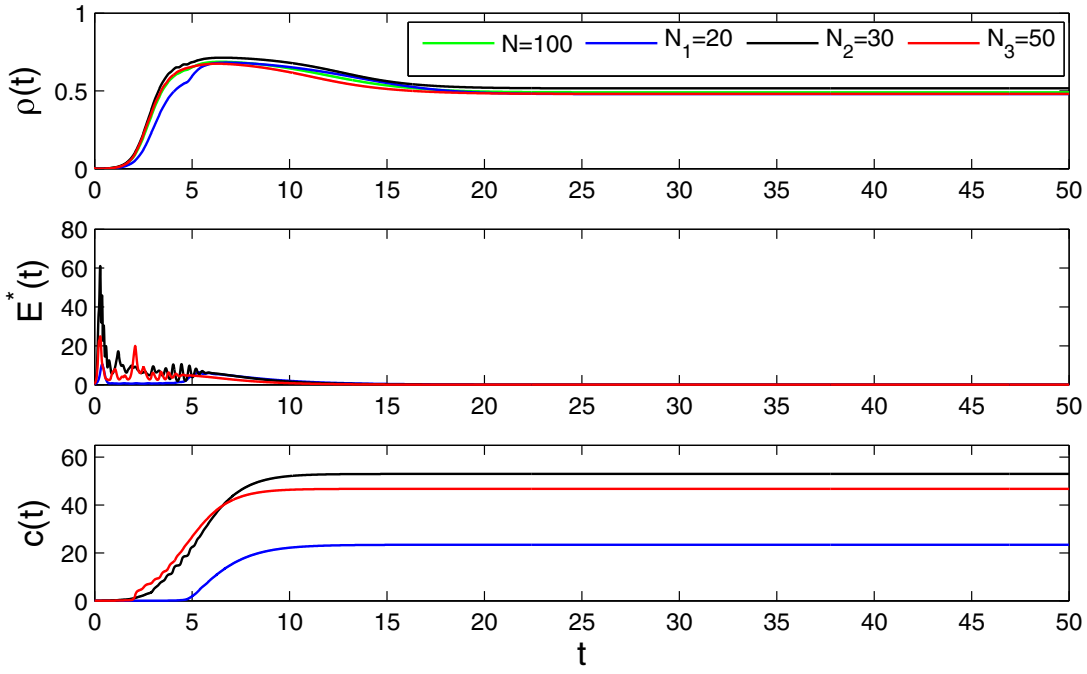

Fig. 4. When the infection rate $\lambda = 0.6 > \lambda_c$, the time evolution of $\rho(t)$, $E^*(t)$ and $c(t)$ in model (4). The steady-state values of the epidemic prevalence are larger. Line colors are similar to that shown in Fig. 2.

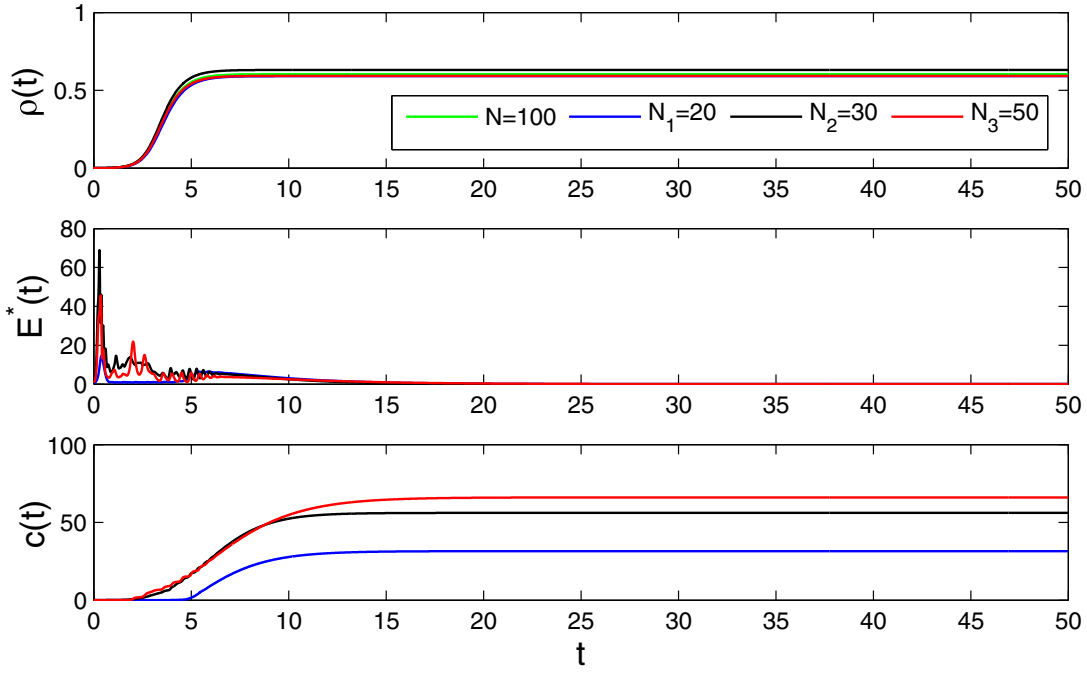

Fig. 5. When the infection rate $\lambda = 0.4 > \lambda_c$ and $\alpha = 1$, the time evolution of $\rho(t)$, $E^*(t)$ and $c(t)$ in model (4). Line colors are similar to that shown in Fig. 2.

the spreading model is λ_c, and there exist no multiple endemic equilibria.

For the cluster synchronization in the network, when the dynamical nodes synchronize each other in each community, however, there exists no synchronization between any two different communities. Now, we define the errors between any two communities for the network as $E_{12}(t) = [x_{i_0}(t) - x_{j_0}(t)]^2, E_{13}(t) = [x_{i_0}(t) - x_{k_0}(t)]^2$, and $E_{23}(t) = [x_{j_0}(t) - x_{k_0}(t)]^2$ for $i_0 \in \{1, \ldots, N_1\}$, $j_0 \in \{N_1 + 1, \ldots, N_1 + N_2\}$, $k_0 \in \{N_1 + N_2 + 1, \ldots, N\}$. Fig. 9 presents the errors of cluster synchronization for the network with three communities when $\lambda = 0.4 > \lambda_c$. In the case, the errors between two communities do not coverage to zero, which imply no synchronization appears between any two different communities.

5. Conclusions

Taking into account the differences in the responses of individuals in different communities, we have established a mathematical model including epidemic spread, behavior information dissemination and community structure.

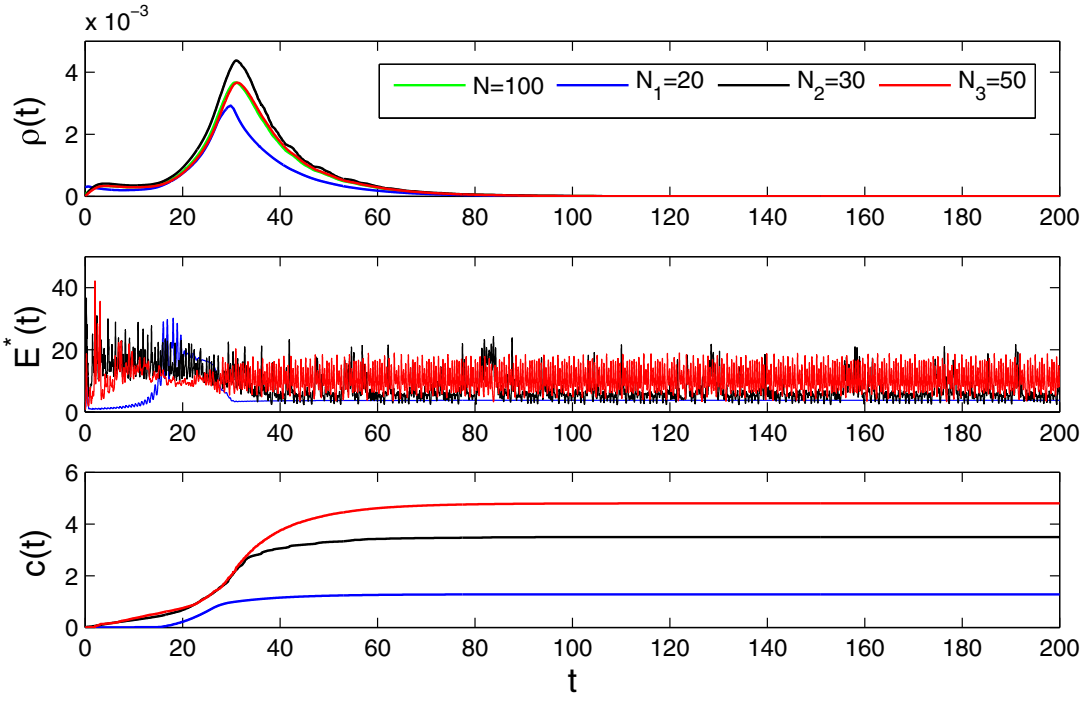

Fig. 6. The time evolution of $\rho(t)$, $E^*(t)$ and $c(t)$ in model (4) with the infection rate $\lambda = 0.145$ and initial value $\rho_3(0) = 0.003$.

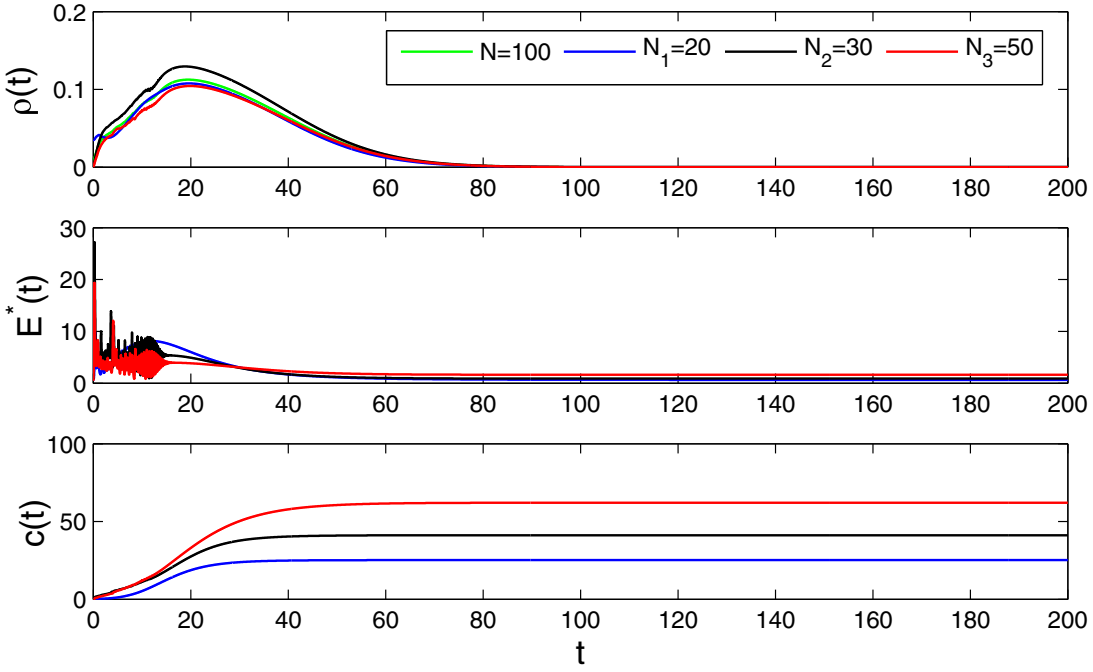

Fig. 7. The time evolution of $\rho(t)$, $E^*(t)$ and $c(t)$ in model (4) with the infection rate $\lambda = 0.155$ and initial value $\rho_3(0) = 0.35$.

By applying comparison principle and Geršgorin theorem, we find out the epidemic threshold of the epidemic spreading network is $\lambda_c = \frac{1}{\alpha\rho(A)}$, which depends on the constant α and the spectral radius $\rho(A)$ of the adjacency matrix A. By constructing suitable Lyapunov functions, we demonstrate that the disease-free equilibrium ρ_0 of the epidemic spreading network is globally asymptotically stable in the feasible region H when $\lambda < \frac{1}{\rho(A)}$, while it is unstable when $\lambda > \lambda_c$, namely, the epidemic spreading network is uniformly persistent in H^0. Furthermore, the cluster synchronization manifold of the dynamical behavior network and the positive equilibrium ρ^* of the epidemic spreading network are both globally asymptotically stable when $\lambda > \lambda_c$. The numerical simulations further show that when $\frac{1}{\rho(A)} < \lambda < \lambda_c$, all the synchronization errors $E^*(t)$ and coupling strengths $c(t)$ converge to nonzero, implying that the epidemic dynamics cannot successfully induce the cluster synchronization of individual behaviors when the disease dies out. And, the simulations also verify that if the dynamical nodes synchronize each other in each community for the cluster synchronization, however, no synchronization appears between any two different communities. Our work is the first one to investigate cluster

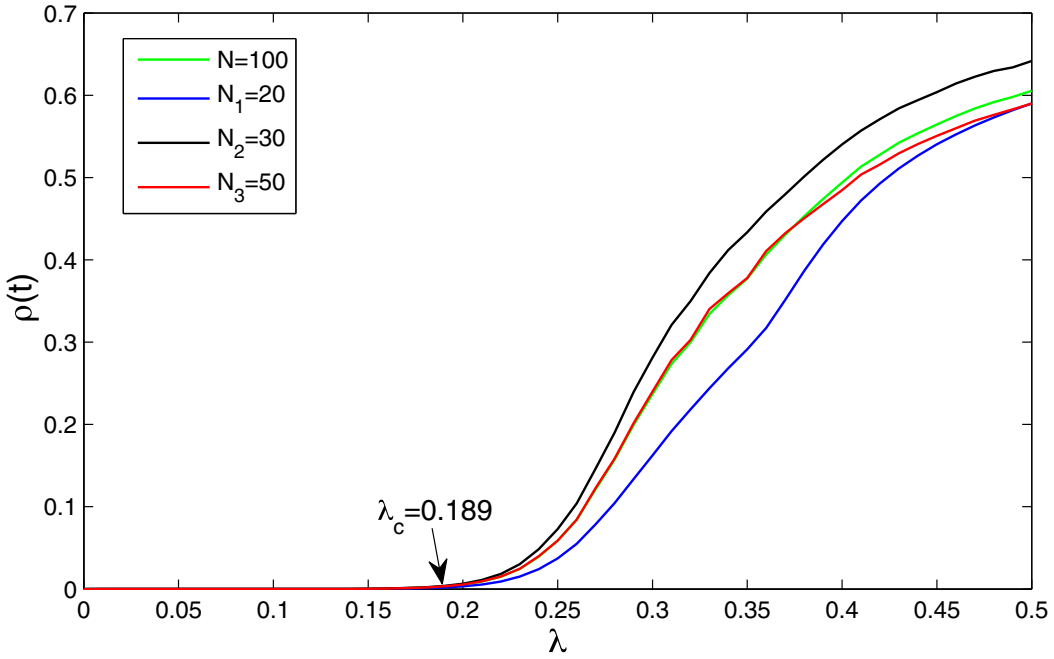

Fig. 8. The epidemic prevalence $\rho(t)$ of the total network and three different communities respect to the effective infection rate λ, respectively.

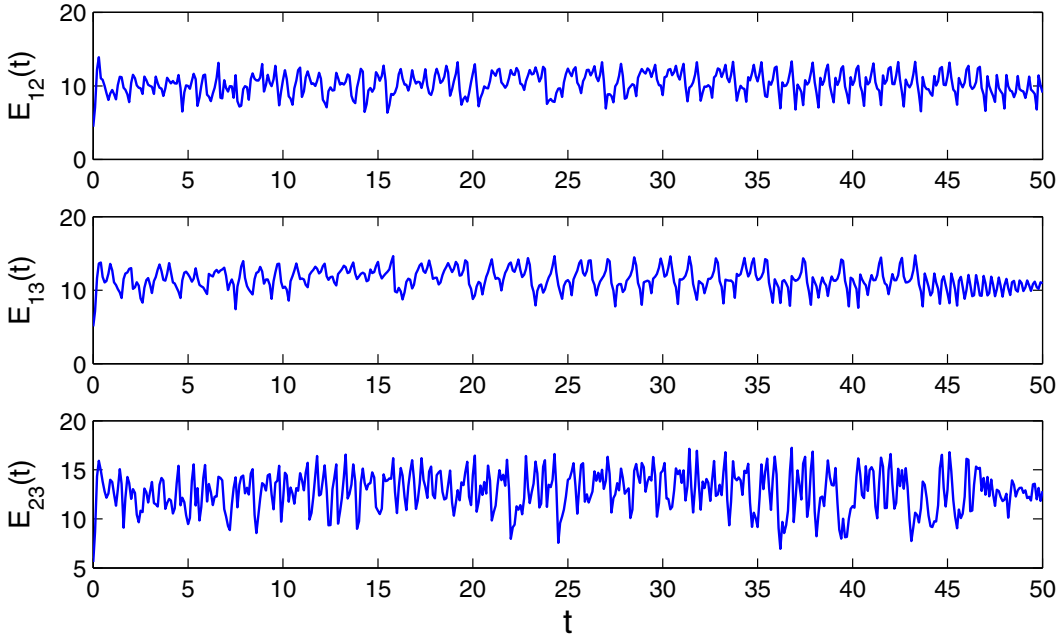

Fig. 9. The errors of cluster synchronization for the network with three communities under $\lambda = 0.4 > \lambda_c$.

synchronization in community networks with nonidentical nodes and epidemic spread, in hope of providing new ideas in the study of cluster synchronization and epidemic spread in community networks.

Acknowledgments

This work was jointly supported by the NSFC grants under Grant nos. 11572181, 11331009 and 61663006. And we thank Wei Zhang from Beijing Jiaotong University for his kind help in numerical simulations.

Appendix A. Proof of Theorem 3

Obviously $S_i(t) + \rho_i(t) = 1$ for $i = 1, 2, \ldots, N$, and we set $\beta_{ij} = \lambda a_{ij}$, then the epidemic spreading network can be rewritten as

$$\dot{S}_i(t) = 1 - S_i - \sum_j \phi_{\sigma_i}(t)\beta_{ij}S_i\rho_j, \tag{22}$$

$$\dot{\rho}_i(t) = -\rho_i + \sum_j \phi_{\sigma_i}(t)\beta_{ij}S_i\rho_j. \tag{23}$$

If $\lambda > \lambda_c$, then the spreading network has an endemic equilibrium ρ^*. Denote the endemic equilibrium by $(\rho_1^*, \rho_2^*, \ldots, \rho_N^*) \in H^0$, $\rho_i^* > 0$ for $i = 1, 2, \ldots, N$. Then, we set $\bar{\beta}_{ij} = \beta_{ij}S_i^*\rho_j^*$, and $S_i^*(t) =$

$1-\rho_i^*(t)$. Hence, define a matrix $\bar{B}$ in which the sum of each column equals zero:

$$\bar{B}=\begin{pmatrix} \sum_{l\neq 1}\bar{\beta}_{1l} & -\bar{\beta}_{21} & \cdots & -\bar{\beta}_{N1} \\ -\bar{\beta}_{12} & \sum_{l\neq 2}\bar{\beta}_{2l} & \cdots & -\bar{\beta}_{N2} \\ \vdots & \vdots & \ddots & \vdots \\ -\bar{\beta}_{1N} & -\bar{\beta}_{2N} & \cdots & \sum_{l\neq N}\bar{\beta}_{Nl} \end{pmatrix}. \tag{24}$$

In order to testify the Theorem, we consider a Lyapunov function $V_0(t)=V_1(t)+V_2(t)$, in which

$$V_1(t)=\sum_{i=1}^{N}\nu_i(S_i-S_i^*\ln S_i+\rho_i-\rho_i^*\ln\rho_i), \tag{25}$$

where $\nu_i>0$ denotes the cofactor of the ith diagonal entry of $\bar{B}$, and $\bar{B}\nu=0$, $\nu=(\nu_1,\ldots,\nu_N)^T$.

Since a unique endemic equilibrium exists, from Eqs. (22) and (23), the derivative of $V_1(t)$ along the solution of system admits

$$\begin{aligned}\dot{V}_1(t)=&\sum_{i=1}^{N}\nu_i\Bigg(1-S_i-\sum_j\phi_{\sigma_i}(t)\beta_{ij}S_i\rho_j\\ &-\frac{S_i^*}{S_i}\left(1-S_i-\sum_j\phi_{\sigma_i}(t)\beta_{ij}S_i\rho_j\right)-\rho_i\\ &+\sum_j\phi_{\sigma_i}(t)\beta_{ij}S_i\rho_j-\frac{\rho_i^*}{\rho_i}\left(\sum_j\phi_{\sigma_i}(t)\beta_{ij}S_i\rho_j-\rho_i\right)\Bigg)\\ =&\sum_{i=1}^{N}\nu_i\Bigg(S_i^*+\alpha\sum_j\beta_{ij}S_i^*\rho_j^*-S_i-\sum_j\phi_{\sigma_i}(t)\beta_{ij}S_i\rho_j\\ &-\frac{S_i^*}{S_i}\left(\alpha\sum_j\beta_{ij}S_i^*\rho_j^*+S_i^*\right)+S_i^*+\sum_j\phi_{\sigma_i}(t)\beta_{ij}S_i^*\rho_j-\rho_i\\ &+\sum_j\phi_{\sigma_i}(t)\beta_{ij}S_i\rho_j-\sum_j\phi_{\sigma_i}(t)\beta_{ij}S_i\rho_j\frac{\rho_i^*}{\rho_i}\\ &+\alpha\sum_j\beta_{ij}S_i^*\rho_j^*\Bigg)\\ =&\sum_{i=1}^{N}\nu_i\Bigg(-S_i^*\left(\frac{S_i}{S_i^*}+\frac{S_i^*}{S_i}-2\right)\\ &+2\alpha\sum_j\beta_{ij}S_i^*\rho_j^*-\alpha\sum_j\beta_{ij}\frac{(S_i^*)^2}{S_i}\rho_j^*\\ &-\sum_j\phi_{\sigma_i}(t)\beta_{ij}S_i\rho_j\frac{\rho_i^*}{\rho_i}+\sum_j\phi_{\sigma_i}(t)\beta_{ij}S_i^*\rho_j-\rho_i\Bigg).\end{aligned} \tag{26}$$

Since $\frac{S_i}{S_i^*}+\frac{S_i^*}{S_i}-2\geq 0$, we get

$$-S_i^*\left(\frac{S_i}{S_i^*}+\frac{S_i^*}{S_i}-2\right)\leq 0, \tag{27}$$

and the equality holds if and only if $S_i=S_i^*$.

Now, we will prove that

$$\sum_{i=1}^{N}\nu_i\left(\sum_{j=1}^{N}\phi_{\sigma_i}(t)\beta_{ij}S_i^*\rho_j-\rho_i\right)\leq\frac{E(t)}{N_0}\sum_{i,j=1}^{N}\nu_i\beta_{ij}S_i^*\rho_j. \tag{28}$$

First, we can obtain

$$\begin{aligned}\sum_{i=1}^{N}\nu_i\left(\sum_{j=1}^{N}\phi_{\sigma_i}(t)\beta_{ij}S_i^*\rho_j-\rho_i\right)&=\sum_{i=1}^{N}\left(\sum_{j=1}^{N}\phi_{\sigma_i}(t)\beta_{ji}S_j^*\nu_j-\nu_i\right)\rho_i\\ &\leq\sum_{i,j=1}^{N}E_{\sigma_i}(t)\nu_j\beta_{ji}S_j^*\rho_i\\ &\quad+\sum_{i=1}^{N}\left(\alpha\sum_{j=1}^{N}\beta_{ji}S_j^*\nu_j-\nu_i\right)\rho_i\\ &\leq\sum_{i,j=1}^{N}\frac{\tilde{E}_{\sigma_i}(t)}{N_{\sigma_i}}\nu_j\beta_{ji}S_j^*\rho_i\\ &\quad+\sum_{i=1}^{N}\left(\alpha\sum_{j=1}^{N}\beta_{ji}S_j^*\nu_j-\nu_i\right)\rho_i\\ &\leq\frac{E(t)}{N_0}\sum_{i,j=1}^{N}\nu_i\beta_{ij}S_i^*\rho_j\\ &\quad+\sum_{i=1}^{N}\left(\alpha\sum_{j=1}^{N}\beta_{ji}S_j^*\nu_j-\nu_i\right)\rho_i,\end{aligned}$$

where $N_0=\min\{N_{\sigma_1},N_{\sigma_2},\ldots,N_{\sigma_N}\}$.

Then, from $\bar{B}\nu=0$ we get

$$\begin{aligned}\alpha\sum_{j=1}^{N}\beta_{ji}S_j^*\rho_i^*\nu_j&=\alpha\sum_{j\neq i}^{N}\bar{\beta}_{ji}\nu_j+\alpha\bar{\beta}_{ii}\nu_i=\alpha\sum_{j\neq i}^{N}\bar{\beta}_{ij}\nu_i+\alpha\bar{\beta}_{ii}\nu_i\\ &=\alpha\sum_{j=1}^{N}\bar{\beta}_{ij}\nu_i=\rho_i^*\nu_i.\end{aligned}$$

Obviously, $\alpha\sum_{j=1}^{N}\beta_{ji}S_j^*\nu_j=\nu_i$ for all i.

Given the above, we get the inequality (28).

According to Eqs. (26)–(28), then applying $\phi_{\sigma_i}(t)\geq\alpha>0$ and $\bar{\beta}_{ij}=\beta_{ij}S_i^*\rho_j^*$, we further get

$$\begin{aligned}\dot{V}_1(t)\leq&\frac{E(t)}{N_0}\sum_{i,j=1}^{N}\nu_i\beta_{ij}S_i^*\rho_j\\ &+\alpha\sum_{i=1}^{N}\nu_i\left(2\sum_{j=1}^{N}\bar{\beta}_{ij}-\sum_{j=1}^{N}\bar{\beta}_{ij}\frac{S_i^*}{S_i}-\sum_{j=1}^{N}\bar{\beta}_{ij}\frac{\rho_jS_i\rho_i^*}{\rho_iS_i^*\rho_j^*}\right)\\ =&\frac{\sum_{i,j=1}^{N}\nu_i\beta_{ij}S_i^*\rho_j}{N_0}\sum_{i=1}^{N}e_i^T(t)e_i(t)\\ &+\alpha\sum_{i,j=1}^{N}\nu_i\bar{\beta}_{ij}\left(2-\frac{S_i^*}{S_i}-\frac{\rho_jS_i\rho_i^*}{\rho_iS_i^*\rho_j^*}\right).\end{aligned} \tag{29}$$

In Ref. Guo et al. (2006), the authors have proven that

$$\sum_{i,j=1}^{N}\nu_i\bar{\beta}_{ij}\left(2-\frac{S_i^*}{S_i}-\frac{\rho_jS_i\rho_i^*}{\rho_iS_i^*\rho_j^*}\right)\leq 0$$

for positive β_{ij}, and the equality holds if and only if $S_i=S_i^*$ and $\rho_i=\rho_i^*$. Then,

$$V_2(t)=\frac{1}{2}e^T(t)(I_N\otimes P)e(t)+\frac{1}{2\beta}\bar{\beta}[C_0-C(t)]^T[C_0-C(t)], \tag{30}$$

where $C_0=(c_0,\ldots,c_0)^T$ is N-dimensional and c_0 is an undetermined constant, $\bar{\beta}=\lambda_2\lambda_{\min}(P\Gamma)/N>0$, and $\lambda_{\min}(P\Gamma)$ denotes the minimal eigenvalue of matrix $P\Gamma$. Therefore,

$$\begin{aligned}\dot{V}_2(t)=&e^T(t)(I_N\otimes P)[F(t)-C(t)(L\otimes\Gamma)e(t)]\\ &-\frac{\bar{\beta}}{\beta}[C_0-C(t)]^T\dot{C}(t)\\ =&e^T(t)(I_N\otimes P)F(t)-C(t)e^T(t)(L\otimes P\Gamma)e(t)\\ &-\frac{\bar{\beta}}{\beta}\sum_{i=1}^{N}(c_0-c_{\sigma_i}(t))\dot{c}_{\sigma_i}(t)\\ =&\sum_{i=1}^{N}e_i^T(t)P[f_{\sigma_i}(x_i(t))-f_{\sigma_i}(s_{\sigma_i}(t))]\end{aligned}$$

$$
\begin{aligned}
&-C(t)e^T(t)(L\otimes P\Gamma)e(t)\\
&+\bar{\beta}\sum_{i=1}^{N}\left(c_{\sigma_i}(t)\rho_{\sigma_i}(t)\sum_{j\in\mathcal{N}_{\sigma_i}}e_j^T(t)e_j(t)\right)\\
&-\bar{\beta}c_0\sum_{i=1}^{N}\left(\rho_{\sigma_i}(t)\sum_{j\in\mathcal{N}_{\sigma_i}}e_j^T(t)e_j(t)\right)\\
&\le \xi\sum_{i=1}^{N}e_i^T(t)e_i(t)-C(t)e^T(t)(L\otimes P\Gamma)e(t)\\
&+\bar{\beta}\sum_{i=1}^{N}\left(c_{\sigma_i}(t)\sum_{j\in\mathcal{N}_{\sigma_i}}e_j^T(t)e_j(t)\right)\\
&-\bar{\beta}c_0\sum_{i=1}^{N}\left(\rho_{\sigma_i}(t)\sum_{j\in\mathcal{N}_{\sigma_i}}e_j^T(t)e_j(t)\right).
\end{aligned}\tag{31}
$$

Now, introducing a transformation $y(t)=(y_1^T(t),\dots,y_N^T(t))^T=(U^T\otimes I_n)e(t)$, we have

$$\sum_{i=1}^{N}e_i^T(t)e_i(t)=\sum_{i=1}^{N}y_i^T(t)y_i(t).$$

Then, we have

$$
\begin{aligned}
&\xi\sum_{i=1}^{N}e_i^T(t)e_i(t)-C(t)e^T(t)(L\otimes P\Gamma)e(t)\\
&+\bar{\beta}\sum_{i=1}^{N}\left(c_{\sigma_i}(t)\sum_{j\in\mathcal{N}_{\sigma_i}}e_j^T(t)e_j(t)\right)\\
&-\bar{\beta}c_0\sum_{i=1}^{N}\left(\rho_{\sigma_i}(t)\sum_{j\in\mathcal{N}_{\sigma_i}}e_j^T(t)e_j(t)\right)\\
&=\xi\sum_{i=1}^{N}e_i^T(t)e_i(t)-C(t)y^T(t)(\Lambda\otimes P\Gamma)y(t)\\
&+\bar{\beta}\sum_{i=1}^{N}\left(c_{\sigma_i}(t)\sum_{j\in\mathcal{N}_{\sigma_i}}e_j^T(t)e_j(t)\right)\\
&-\bar{\beta}c_0\sum_{i=1}^{N}\left(\rho_{\sigma_i}(t)\sum_{j\in\mathcal{N}_{\sigma_i}}e_j^T(t)e_j(t)\right)\\
&=\xi\sum_{i=1}^{N}e_i^T(t)e_i(t)-\sum_{i=1}^{N}c_{\sigma_i}(t)\lambda_i y_i^T(t)P\Gamma y_i(t)\\
&+\bar{\beta}\sum_{i=1}^{N}\left(c_{\sigma_i}(t)\sum_{j\in\mathcal{N}_{\sigma_i}}e_j^T(t)e_j(t)\right)\\
&-\bar{\beta}c_0\sum_{i=1}^{N}\left(\rho_{\sigma_i}(t)\sum_{j\in\mathcal{N}_{\sigma_i}}e_j^T(t)e_j(t)\right)\\
&\le\xi\sum_{i=1}^{N}e_i^T(t)e_i(t)-\lambda_2\lambda_{\min}(P\Gamma)\sum_{i=1}^{N}c_{\sigma_i}(t)y_i^T(t)y_i(t)\\
&+\bar{\beta}N\sum_{i=1}^{N}c_{\sigma_i}(t)e_i^T(t)e_i(t)\\
&-\bar{\beta}c_0\sum_{i=1}^{N}\left(\rho_{\sigma_i}(t)\sum_{j\in\mathcal{N}_{\sigma_i}}e_j^T(t)e_j(t)\right)\\
&=\xi\sum_{i=1}^{N}e_i^T(t)e_i(t)-\lambda_2\lambda_{\min}(P\Gamma)\sum_{i=1}^{N}c_{\sigma_i}(t)e_i^T(t)e_i(t)\\
&+\bar{\beta}N\sum_{i=1}^{N}c_{\sigma_i}(t)e_i^T(t)e_i(t)\\
&-\bar{\beta}c_0\sum_{i=1}^{N}\left(\rho_{\sigma_i}(t)\sum_{j\in\mathcal{N}_{\sigma_i}}e_j^T(t)e_j(t)\right)\\
&=\xi\sum_{i=1}^{N}e_i^T(t)e_i(t)+[\bar{\beta}N-\lambda_2\lambda_{\min}(P\Gamma)]\sum_{i=1}^{N}c_{\sigma_i}(t)e_i^T(t)e_i(t)\\
&-\bar{\beta}c_0\sum_{i=1}^{N}\left(\rho_{\sigma_i}(t)\sum_{j\in\mathcal{N}_{\sigma_i}}e_j^T(t)e_j(t)\right)\\
&\le\xi\sum_{i=1}^{N}e_i^T(t)e_i(t)-\bar{\beta}c_0\hat{\rho}(t)\sum_{i=1}^{N}\sum_{j\in\mathcal{N}_{\sigma_i}}e_j^T(t)e_j(t)\\
&\le\xi\sum_{i=1}^{N}e_i^T(t)e_i(t)-\bar{\beta}c_0\hat{\rho}(t)\sum_{i=1}^{N}e_i^T(t)e_i(t)\\
&=[\xi-\bar{\beta}c_0\hat{\rho}(t)]\sum_{i=1}^{N}e_i^T(t)e_i(t),
\end{aligned}
$$

where $\hat{\rho}(t)=\min\{\rho_{\sigma_1}(t),\rho_{\sigma_2}(t),\dots,\rho_{\sigma_N}(t)\}$.

If $\lambda>\lambda_c$ for system (4), there exists a constant $\bar{\rho}\in(0,1]$, such that $\lim_{t\to+\infty}\hat{\rho}(t)=\bar{\rho}$. By choosing $\varepsilon\in(0,\bar{\rho})$ and $t_0>0$, so $\hat{\rho}(t)>\bar{\rho}-\varepsilon$ for all $t>t_0$. If $t>t_0$, we have

$$\dot{V}_2(t)\le[\xi-\bar{\beta}c_0(\bar{\rho}-\varepsilon)]\sum_{i=1}^{N}e_i^T(t)e_i(t).\tag{32}$$

Thus, by selecting an adequately large constant c_0 make $\dot{V}_2(t)\le 0$. Furthermore, we can get the following inequalities

$$
\begin{aligned}
&\frac{\lambda_{\min}(P)}{2}\sum_{i=1}^{N}e_i^T(t)e_i(t)+\frac{\bar{\beta}}{2\beta}\sum_{i=1}^{N}(c_0-c_{\sigma_i}(t))^2\le V_2(t)\le\\
&\frac{\lambda_{\max}(P)}{2}\sum_{i=1}^{N}e_i^T(t)e_i(t)+\frac{\bar{\beta}}{2\beta}\sum_{i=1}^{N}(c_0-c_{\sigma_i}(t))^2.
\end{aligned}
$$

So, the function $V_2(t)$ has infinitesimal upper bound and is infinitely large.

According to the above discussions, we have

$$
\begin{aligned}
\dot{V}_0(t)\le&\left[\frac{\sum_{i,j=1}^{N}\nu_i\beta_{ij}S_i^*\rho_j}{N_0}+\xi-\frac{\lambda_2\lambda_{\min}(P\Gamma)}{N}c_0(\bar{\rho}-\varepsilon)\right]\\
&\times\sum_{i=1}^{N}e_i^T(t)e_i(t).
\end{aligned}\tag{33}
$$

By selecting an adequately large constant c_0, we have $\dot{V}_0(t)\le 0$. By the LaSalle's invariance principle, we obtain the unique endemic equilibrium ρ^* of the spreading network is globally asymptotically stable in H^0, that is, the synchronization manifold Ψ of the dynamical network is also globally asymptotically stable. □

References

Arenas, A., Diaz-Guilera, A., Guimera, R., 2001. Communication in networks with hierarchical branching. Phys. Rev. Lett. 86 (14), 3196.

Barabási, A.L., 2007. Scale-free networks: a decade and beyond. Science 316 (5827), 1036–1039.

Barabási, A.L., Albert, R., 1999. Emergence of scaling in random networks. Science 286 (5439), 509–512.

Barabási, A.L., Bonabeau, E., 2003. Scale-free networks. Sci. Am. 288 (5), 60–69.

Boccaletti, S., Latora, V., Moreno, Y., Chavez, M., Hwang, D.U., 2006. Complex networks: structure and dynamics. Phys. Rep. 424 (4–5), 175–308.

Boguñá, M.B., Castellano, C., Pastor-Satorras, R., 2013. Nature of the epidemic threshold for the susceptible-infected-susceptible dynamics in networks. Phys. Rev. Lett. 111 (6), 068701.

Boguñá, M., Pastor-Satorras, R., Vespignani, A., 2003. Absence of epidemic threshold in scale-free networks with degree correlations. Phys. Rev. Lett. 90 (2), 028701.
Cai, Y.L., Kang, Y., Banerjee, M., Wang, W.M., 2015. A stochastic SIRS epidemic model with infectious force under intervention strategies. J. Differ. Equ. 259 (12), 7463–7502.
Chu, X.W., Guan, J.H., Zhang, Z.Z., Zhou, S.G., 2009. Epidemic spreading in weighted scale-free networks with community structure. J. Stat. Mech.-Theory E. 2009 (07), P07043.
Dharmaweera, M.N., Parthiban, R., Sekercioglu, Y.A., 2015. Toward a power-efficient backbone network: the state of research. IEEE Commun. Surv. Tut. 17 (1), 198–227.
Duarte, N.C., Becker, S.A., Jamshidi, N., et al., 2007. Global reconstruction of the human metabolic network based on genomic and bibliomic data. P. Natl. Acad. Sci. USA 104 (6), 1777–1782.
Funk, S., Gilad, E., Watkins, C., Jansen, V.A.A., 2009. The spread of awareness and its impact on epidemic outbreaks. P. Natl. Acad. Sci. USA 106 (16), 6872–6877.
Funk, S., Salathé, M., Jansen, V.A.A., 2010. Modelling the influence of human behaviour on the spread of infectious diseases: a review. J. R. Soc. Interface, 20100142.
Garas, A., Argyrakis, P., Rozenblat, C., Tomassini, M., Havlin, S., 2010. Worldwide spreading of economic crisis. New J. Phys. 12 (2), 185–188.
Girvan, M., Newman, M.E.J., 2002. Community structure in social and biological networks. P. Natl. Acad. Sci. USA 99 (12), 7821–7826.
Golubitsky, M., Stewart, I., 2006. Nonlinear dynamics of networks: the groupoid formalism. B. Am. Math. Soc. 43 (3), 305–364.
Guo, H.B., Li, M.Y., Shuai, Z.S., 2006. Global stability of the endemic equilibrium of multigroup SIR epidemic models. Can. Appl. Math. Q. 14 (259), 259–284.
Huang, W., Li, C.G., 2007. Epidemic spreading in scale-free networks with community structure. J. Stat. Mech.-Theory E. 2007 (01), P01014.
Kan, J.Q., Zhang, H.F., 2017. Effects of awareness diffusion and self-initiated awareness behavior on epidemic spreading-an approach based on multiplex networks. Commun. Nonlinear Sci. Numer. Simul. 44, 193–203.
Keeling, M.J., Eames, K.T.D., 2005. Networks and epidemic models. J. R. Soc. Interface 2 (4), 295–307.
Khan, Z.U., Hayat, M., Khan, M.A., 2015. Discrimination of acidic and alkaline enzyme using chou's pseudo amino acid composition in conjunction with probabilistic neural network model. J. Theor. Biol. 365c (6), 197–203.
Kumar, A., Srivastava, P.K., Takeuchi, Y., 2017. Modeling the role of information and limited optimal treatment on disease prevalence. J. Theor. Biol. 414 (7), 103–119.
Li, K.Z., Fu, X.C., Small, M., Ma, Z.J., 2011. Adaptive mechanism between dynamical synchronization and epidemic behavior on complex networks. Chaos 21 (3), 033111.
Li, K.Z., Ma, Z.J., Jia, Z., Small, M., Fu, X.C., 2012. Interplay between collective behavior and spreading dynamics on complex networks. Chaos 22 (4), 043113.
Liebovitch, L.S., Schwartz, I.B., 2003. Information flow dynamics and timing patterns in the arrival of email viruses. Phys. Rev. E 68 (1), 017101.
Liu, Z.H., Lai, Y.C., Ye, N., 2003. Propagation and immunization of infection on general networks with both homogeneous and heterogeneous components. Phys. Rev. E 67 (3), 031911.
Lozano, S., Arenas, A., Sánchez, A., 2008. Mesoscopic structure conditions the emergence of cooperation on social networks. PLoS One 3 (4), e1892.
Moreno, Y., Nekovee, M., Pacheco, A.F., 2004. Dynamics of rumor spreading in complex networks. Phys. Rev. E 69 (6), 066130.
Newman, M.E.J., 2002. Spread of epidemic disease on networks. Phys. Rev. E 66 (1), 016128.
Newman, M.E.J., 2006. Modularity and community structure in networks. P. Natl. Acad. Sci. USA 103 (23), 8577–8582.
Newman, M.E.J., 2012. Communities, modules and large-scale structure in networks. Nat. Phys. 8 (1), 25–31.
Newman, M.E.J., Forrest, S., Balthrop, J., 2002. Email networks and the spread of computer viruses. Phys. Rev. E 66 (3), 035101.
Ohira, T., Sawatari, R., 1998. Phase transition in a computer network traffic model. Phys. Rev. E 58 (1), 193.
Orosz, G., Wilson, R.E., Stépán, G., 2010. Traffic jams: dynamics and control. Phil. Trans. R. Soc. A 368 (1928), 4455–4479.
Sun, M.F., Lou, Y.J., Duan, J.Q., Fu, X.C., 2017. Behavioral synchronization induced by epidemic spread in complex networks. Chaos 27 (6), 063101.
Verelst, F., Willem, L., Beutels, P., 2016. Behavioural change models for infectious disease transmission: a systematic review (2010–2015). J. R. Soc. Interface 13 (125), 20160820.
Vidal, M., Cusick, M.E., Barabási, A.L., 2011. Interactome networks and human disease. Cell 144 (6), 986–995.
Vitali, S., Glattfelder, J., Battiston, S., 2011. The network of global corporate control. PLoS One 6 (10), e25995.
Wang, L.N., Sun, M.F., Chen, S.S., Fu, X.C., 2016. Epidemic spreading on one-way-coupled networks. Physica A 457 (1), 280–288.
Watts, D.J., 2007. A 21st century science. Nature 445 (7127), 489.
Wu, Q.C., Fu, X.C., Small, M., Xu, X.J., 2012. The impact of awareness on epidemic spreading in networks. Chaos 22 (1), 013101.
Zanette, D.H., 2002. Dynamics of rumor propagation on small-world networks. Phys. Rev. E 65 (4), 041908.
Zhang, F.Z., 2010. Matrix Theory: Basic Results and Techniques (Universitext). Springer, New York, p. 68.
Zhang, H.F., Shu, P.P., Wang, Z., Tang, M., Small, M., 2017. Preferential imitation can invalidate targeted subsidy policies on seasonal-influenza diseases. Appl. Math. Comput. 294 (1), 332–342.
Zhang, H.F., Xie, J.R., Tang, M., Lai, Y.C., 2014. Suppression of epidemic spreading in complex networks by local information based behavioral responses. Chaos 24 (4), 043106.